Electronic Supplementary Information

Efficient Electrochemical N_2 Fixation by Doped-Oxygen Induced Phosphorus Vacancy Defects on Copper Phosphide Nanosheets

Meng Jin,[a,b] Xian Zhang,[a] Miaomiao Han,[a] Haojie Wang,[a] Guozhong Wang[a] and Haimin Zhang*[a]*

[a]Key Laboratory of Materials Physics, Centre for Environmental and Energy Nanomaterials, Anhui Key Laboratory of Nanomaterials and Nanotechnology, CAS Center for Excellence in Nanoscience, Institute of Solid State Physics, Chinese Academy of Sciences, Hefei 230031, China.

[b]University of Science and Technology of China, Hefei 230026, China.

*Corresponding authors: zhangxian158229@163.com; zhanghm@issp.ac.cn.

Experimental Section

Chemicals and materials: Na_2SO_4 and $(NH_4)_2SO_4$ were purchased from Aladdin Reagent Company. Commercial Cu powder, Cu_2O powder, $CuCl_2•2H_2O$, potassium hydroxide (KOH), and red phosphorus were purchased from Shanghai Sinopharm Chemical Regent Co. Ltd. All the chemicals were used in experiments without further treatment and purification. The commercial carbon fiber cloth (CFC) was provided from Shanghai Hesen Electric Co. LTD

***Synthesis of reduced oxygen-doped Cu_3P/CFC (RO-Cu_3P/CFC) and Cu_3P/CFC electrodes*.** The self-supported copper phosphides on carbon fiber cloth (CFC) were fabricated through a facile vapor-phase hydrothermal (VPH) route, similar with previous work reported by us. A schematic illustration of the fabrication of O-Cu_3P/CFC and Cu_3P/CFC electrodes was shown in Fig. 1a. Firstly, the CFC (2.0×1.0 cm^2) was immersed into HCl (5 M) solution for 48 h to increase the surface functional groups (*e.g.*, -OH, -COOH). After adequately washing with ethyl alcohol and deionized water, the pre-treated CFC was immersed into 6.0 mM Cu^{2+} ($CuCl_2$) aqueous solution for 24 h to obtain Cu^{2+}-adsorbed CFC (Cu^{2+}/CFC). After freeze-drying for 12 h, the Cu^{2+}/CFC was used as precursor and placed on a Teflon holder (100 mL) containing 0.35 g of red phosphorus and 20 mL of 3.0 M NaOH solution to perform vapor-phase hydrothermal (VPH) reaction. The VPH reaction was operated at 220 °C for 0.1 h, 0.2 h, 0.3 h, and 0.6 h, respectively. After that, the obtained product for 0.1 h, 0.2 h, 0.3 h, and 0.6 h, were denoted as O-Cu_3P/CFC-0.1, O-Cu_3P/CFC-0.2, O-Cu_3P/CFC and Cu_3P/CFC, respectively. The RO-Cu_3P/CFC was

obtained by further electrochemical reduction of O-Cu_3P in a N_2-saturated electrolyte solution.

Preparation of Cu/CFC and Cu_2O/CFC electrodes. To fabricate Cu/CFC and Cu_2O/CFC electrodes, 4.0 mg commercial Cu or Cu_2O nanoparticles, 300 μL of isopropanol and 10 μL of Nafion ionomer solution (5.0 wt.%) were first mixed under ultrasonic treatment for 30 min to achieve homogeneous catalyst ink solution, and then the catalyst ink was completely coated onto carbon fiber cloth substrate, followed by drying at 60 °C for 5 h in vacuum.

Material characterization. The crystalline structures of electrodes were identified by X-ray diffraction analysis (XRD, Philips X'pert PRO) using Nifiltered monochromatic CuKa radiation (λKα1 = 1.5418 Å) at 40 kV and 40 mA. The morphology and microstructure of electrodes were characterized by field emission scanning electron microscopy (FESEM, Quanta 200FEG) and transmission electron microscopy (TEM, JEOL 2010) with an energy dispersive X-ray spectrometer (EDS Oxford, Link ISIS). X-ray photoelectron spectroscopy (XPS) analysis was performed on an ESCALAB 250 X-ray photoelectron spectrometer (Thermo, America) equipped with Al $K\alpha_{1,2}$ monochromatized radiation at 1486.6 eV X-ray source. Raman spectra of the samples were recorded on a LabRAM HR800 confocal microscope Raman system (Horiba Jobin Yvon) using an Ar ion laser operating at 532 nm. Cu $L_{3,2}$ edge X-ray absorption spectra (XAS) were performed at BL12B-a beamline of NSRL in the total electron yield (TEY) mode.

Electrochemical measurements. The electrocatalytic NRR performance of the

as-prepared electrodes was evaluated in a traditional three-electrode configured two-compartment reaction system on a CHI760D (CH Instruments, Inc., Shanghai, China) electrochemical workstation, and Ag/AgCl (3.0 M KCl solution) and Pt mesh as the reference and counter electrode, respectively. For the electrocatalytic NRR experiments, the Na_2SO_4 electrolyte (pH=3, adjusted by H_2SO_4) was continuously bubbled with N_2 at a flow rate of 40 mL min^{-1} for at least 30 min before all experiments, and then the N_2 flow rate was decreased to 15 mL min^{-1} during the N_2 reduction reaction. Then evaluated for the NRR under identical experimental conditions. The electrolyte volume used in each compartment was 40 mL and the electrode area used in our work was 1.0 cm^2. In this work, all measured potentials were calibrated to be vs. reversible hydrogen electrode (RHE) according to the following equation:

$$E_{\mathrm{RHE}} = E_{\mathrm{Ag/AgCl}} + 0.059\mathrm{pH} + E^{\circ}_{\mathrm{Ag/AgCl}}$$

where E_{RHE} is the converted potential (V) vs. RHE, $E^{o}_{Ag/AgCl}$= 0.197 V at 25 °C, and $E_{Ag/AgCl}$ is the experimentally measured potential against Ag/AgCl reference electrode.

Nafion 117 membrane pretreatment procedures. Firstly, the Nafion 117 membrane was treated at 80 ^{o}C in 5% hydrogen peroxide for 1 h, and then soaked in deionized water for half an hour. Then boil the Nafion 117 membrane in 5% dilute sulfuric acid (mass ratio) at 80 ^{o}C for 1 h. Finally, soak the membrane in deionized water for 0.5 h.

Determination of NH_3. The yield of ammonia produced in the electrolyte during

the NRR was measured by the indophenol blue spectrophotometry method on UV-Vis 2700 spectrophotometer (Shimadzu, Japan). In detail, 5.0 mL of post-NRR electrolyte was diluted with 5.0 mL of 0.1 M Na_2SO_4. Then, 500 μL of 0.55 M NaOH solution (contains 5.0 wt.% salicylic acid and 5.0 wt.% sodium citrate), 100 μL of $C_5FeN_6Na_2O$ (10 g L^{-1}) and 100 μL of 0.05 M NaClO were successively added to the above pre-diluted electrolyte with rapid stirring for several times at room temperature. The UV-Vis absorption spectrum was measured after the above solution incubating for 1 h at room temperature with the absorbance at a wavelength of 695 nm. The standard curve of $(NH_4)_2SO_4$ concentration-absorbance were calibrated through standard ammonia chloride solution in 0.1 M Na_2SO_4 solution (pH=3, adjusted by H_2SO_4) containing color reagent with a series of $(NH_4)_2SO_4$ concentration as a function of absorbance at a wavelength of 695 nm. The obtained calibration curve was used to calculate the ammonia concentration.

Determination of N_2H_4. The Watt and Chrisp method was applied to analyze the N_2H_4 yield in the electrolyte. The p-$C_9H_{11}NO$ (5.99 g), HCl (30 mL), and C_2H_5OH (300 mL) were first mixed as a color reagent. In detail, 1.0 mL of post-NRR electrolyte was acidized with 9.0 mL of 1.0 M HCl solution, and then added 5.0 mL of color reagent with rapid stirring for several times at room temperature. After incubating for 20 min, the mixture was measured on an UV-Vis 2700 spectrophotometer with absorbance at a wavelength of 455 nm. The obtained calibration curve was used to calculate the hydrazine concentration.

Stability test. The NRR performance stability is measured in two ways. The first

is the cyclic testing method: the recycling NH_3 and N_2H_4 yield test of the RO-Cu_3P/CFC electrode at -0.3 V (vs. RHE) in N_2-saturated electrolyte solution with the reaction time of 2 h for each recycling experiment. Another is a long-term testing method: measure the NH_3 and N_2H_4 yield of the RO-Cu_3P/CFC during the durability measurement for 10 h.

Computational Details

In the present work all calculations were performed by using density function theory (DFT) as implemented in the Vienna ab initio simulation package (VASP). The electronic exchange-correlation energy was treated by the generalized-gradient approximation (GGA) of Perdew-Burke-Ernzerh of (PBE). The electron-ion interactions are described by projector augmented wave (PAW) potentials. The kinetic energy cutoff for the plane-wave expansion is set to 450 eV, and the Monkhorst-Pack k-point mesh of 2 × 2 × 1 was found to provide sufficient accuracy in the integration of the Brillouin zone. For the geometry optimization, the convergence criteria of electronic were 10^{-4} eV and ionic iterations was smaller than 0.05 eV/Å, respectively. On the basis of the optimized unit cells, the six-layer 2 × 2 (1–10) surface was constructed. The top three layers of the surface were allowed to relax together with adsorbates, while the bottom three layers were fixed to present the bulk properties. A vacuum gap of 15 Å was imposed to avoid interactions between periodic images. For the NRR reaction pathways, all the Gibbs free energy values were referenced to the computational hydrogen electrode (CHE) model which was proposed by Nørskov and co-workers. The H^+/e^- pair chemical potential is equal to

half of the gas-phase H_2 under standard reaction conditions (pH = 0, T =298.15 K, P =1 atm)

The elementary steps involved in the electrochemical reaction of nitrogen reduction reaction (NRR) in acidic condition are as follows:

$N_2 + * \rightarrow *N_2$

$*N_2 + H^+ + e^- \rightarrow *N_2H$

$*N_2H + H^+ + e^- \rightarrow *NHNH$

$*NHNH + H^+ + e^- \rightarrow *NHNH_2$

$*NHNH_2 + H^+ + e^- \rightarrow *NH_2NH_2$

$*NH_2NH_2 + H^+ + e^- \rightarrow *NH_2 + NH_3$

$*NH_2 + H^+ + e^- \rightarrow *NH_3$

$*NH_3 \rightarrow NH_3 + *$

Table S1. Calculated zero point energies (ZPE) and entropy of different adsorption species, where the * denotes the adsorption site (T=298.15 K). The entropies of gas phase are obtained from the NIST database.

Adsorption species	E_{ZPE}(ev)	TS(ev)
N_2	0.155	0.593
*NH_2-vacancy	0.700	0.082
*NH_2-doped	0.685	0.076
*NH_3-vacancy	1.010	0.136
*NH_3-doped	1.008	0.160
*N_2-vacancy	0.188	0.140
*N_2-doped	0.189	0.203
*N_2-doped-2O	0.174	0.259
*N=NH-vacancy	0.482	0.152
*N=NH-doped	0.441	0.154
*N=NH-doped-2O	0.490	0.126
*NH-NH-vacancy	0.807	0.196
*NH-NH-doped	0.784	0.174
*NH-NH_2-vacancy	1.142	0.196
*NH-NH_2-doped	1.092	0.144
*NH_2-NH_2-vacancy	1.467	0.232
*NH_2-NH_2-doped	1.462	0.252
NH_3	0.591	0.597

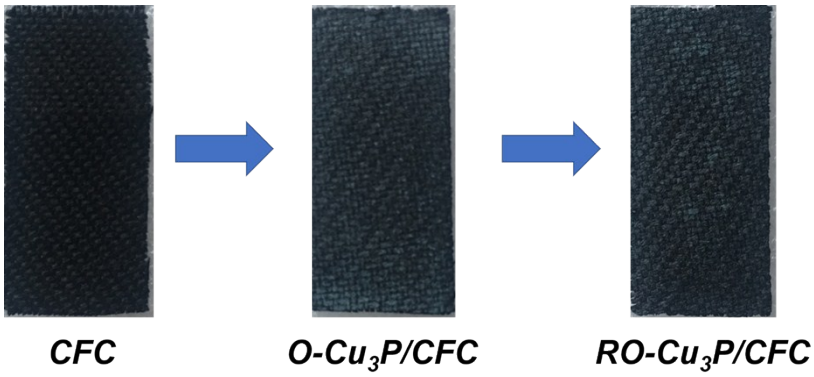

Fig. S1 The photographs of the as-prepared electrodes.

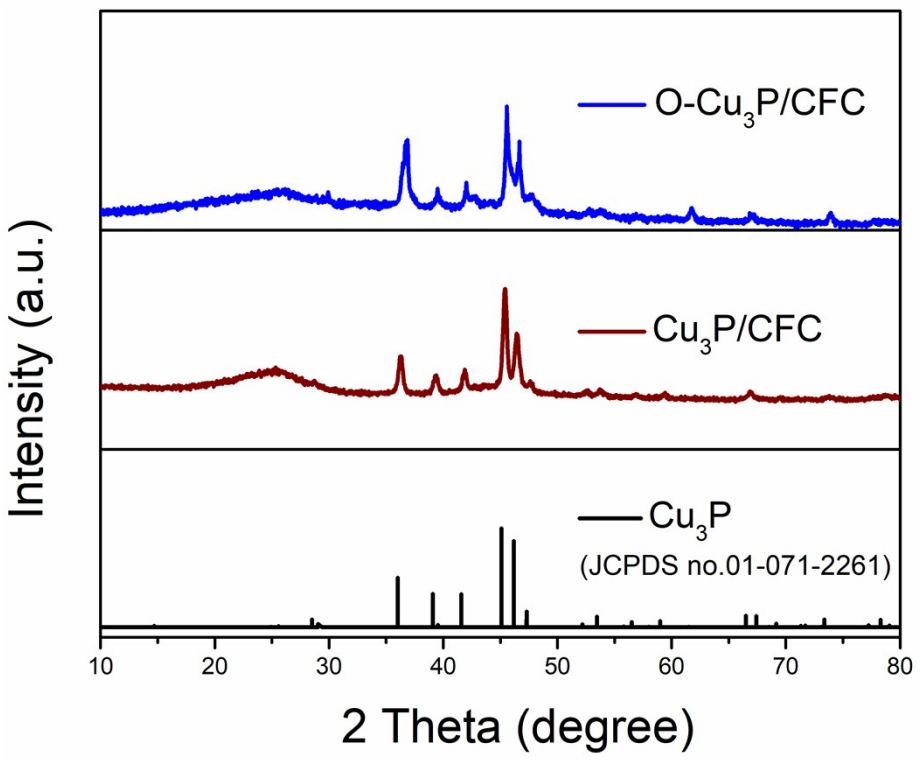

Fig. S2 The XRD patterns of as prepared O-Cu_3P/CFC and Cu_3P/CFC.

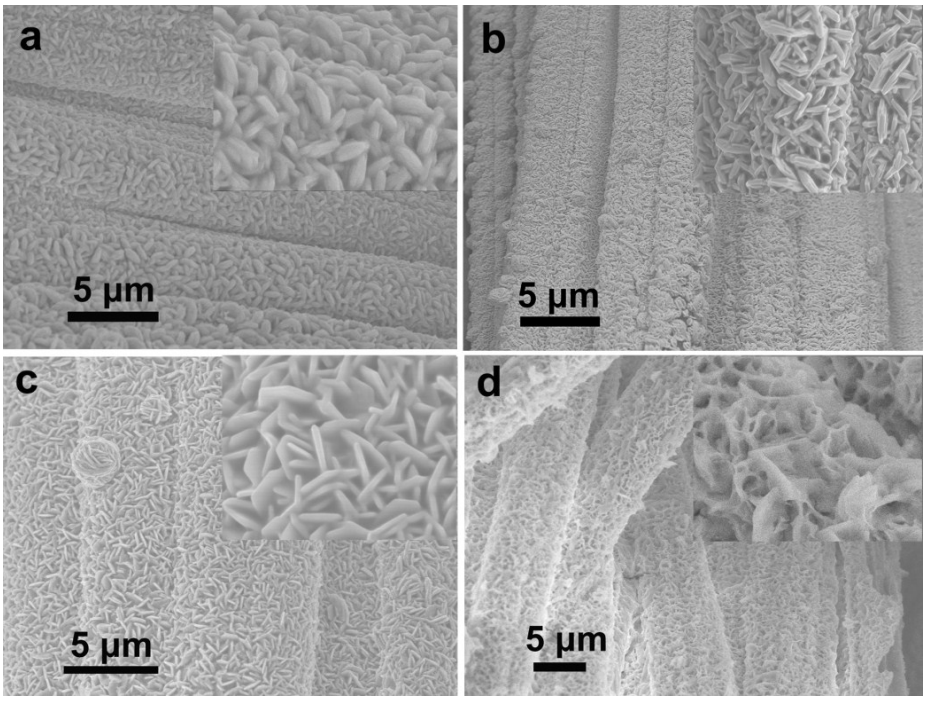

Fig. S3 The SEM images of Cu phosphide prepared with different VPH time (a) 0.1 h, (b) 0.2 h, (c) 0.3 h and (d) 0.6 h. Those electrodes can be denoted as O-Cu_3P/CFC-0.1, O-Cu_3P/CFC-0.2, O-Cu_3P/CFC and Cu_3P/CFC, respectively.

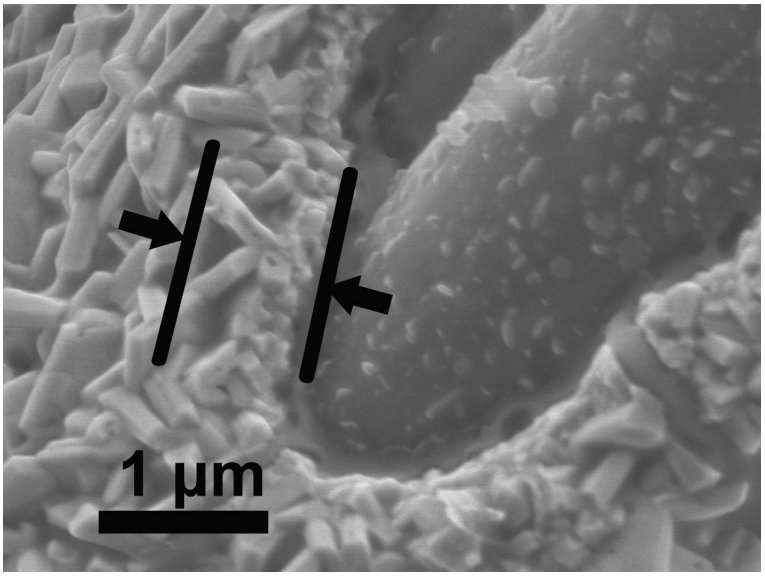

Fig. S4 The SEM images of RO-Cu_3P electrode.

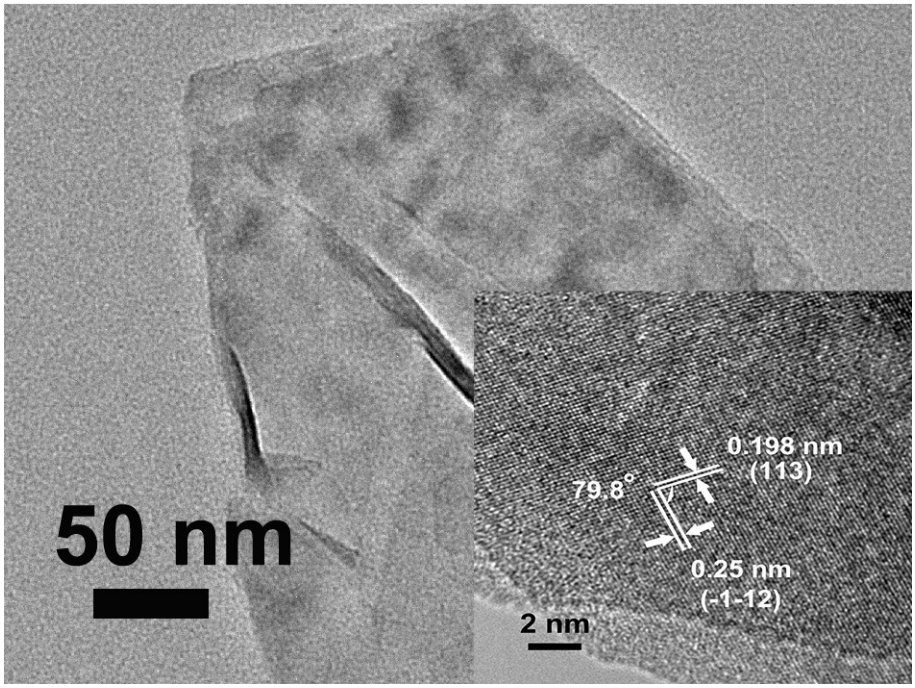

Fig. S5 TEM and HRTEM images of Cu_3P/CFC.

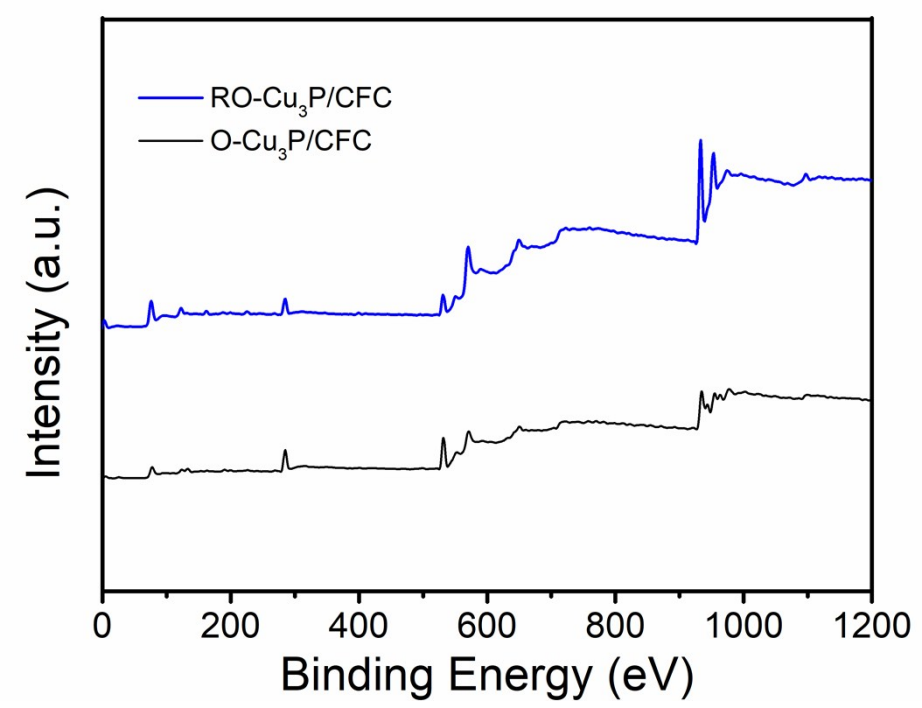

Fig. S6 XPS survey spectra of RO-Cu_3P/CFC and O-Cu_3P/CFC.

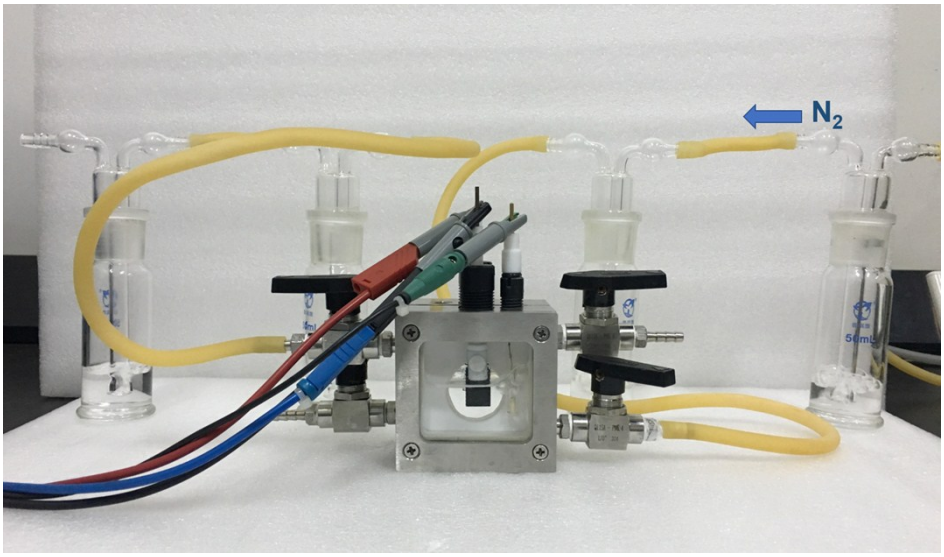

Fig. S7 The photograph of H-type reactor with two compartments separated by proton-conductive Nafion 117 membrane and gas absorption devices.

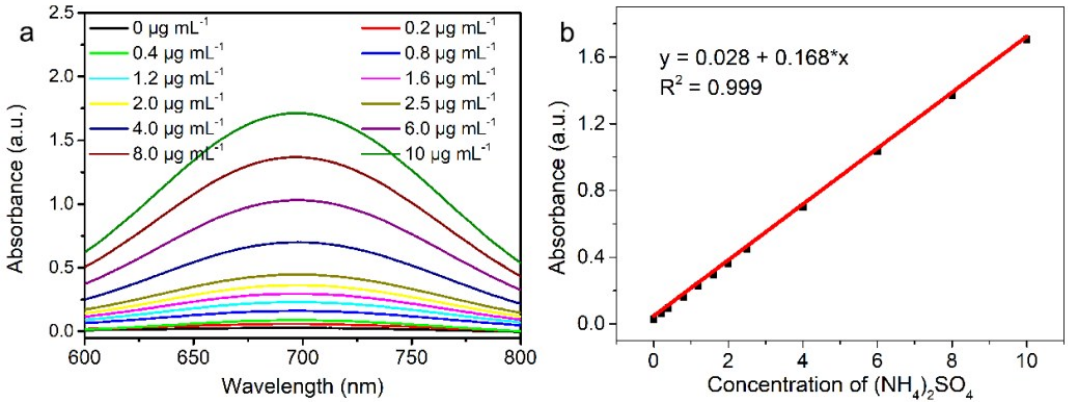

Fig. S8 a) UV-Vis absorbance spectra of the indophenol blue indicator with different concentrations of NH_4^+ ions in 0.1 M Na_2SO_4 after incubating for 1 h at room temperature. b) Calibration curve obtained from the absorbance at a wavelength of 690 nm as a function of the various NH_4Cl concentrations.

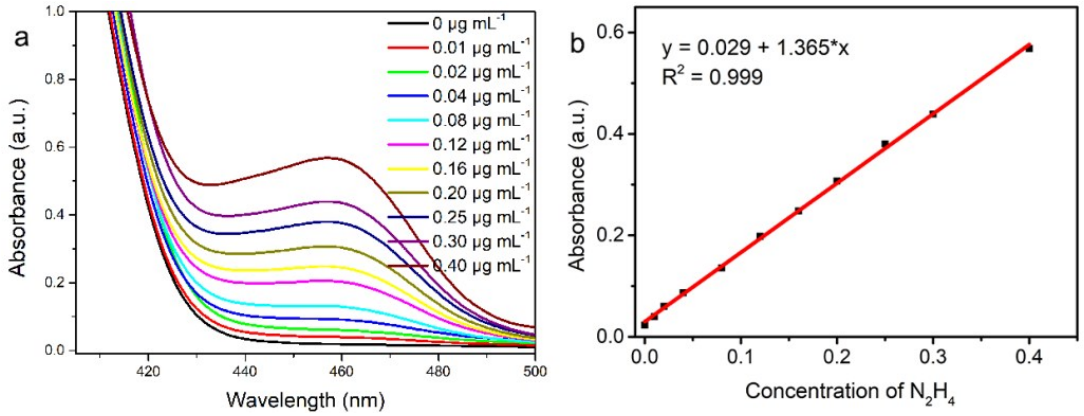

Fig. S9 a) UV-Vis absorbance spectra obtained by the Watt and Chrisp method with different concentrations of $N_2H_4 \cdot H_2O$ in 1.0 M HCl after incubating for 20 min at room temperature, (b) Calibration curve obtained from the absorbance at a wavelength of 455 nm as a function of the various concentrations of N_2H_4.

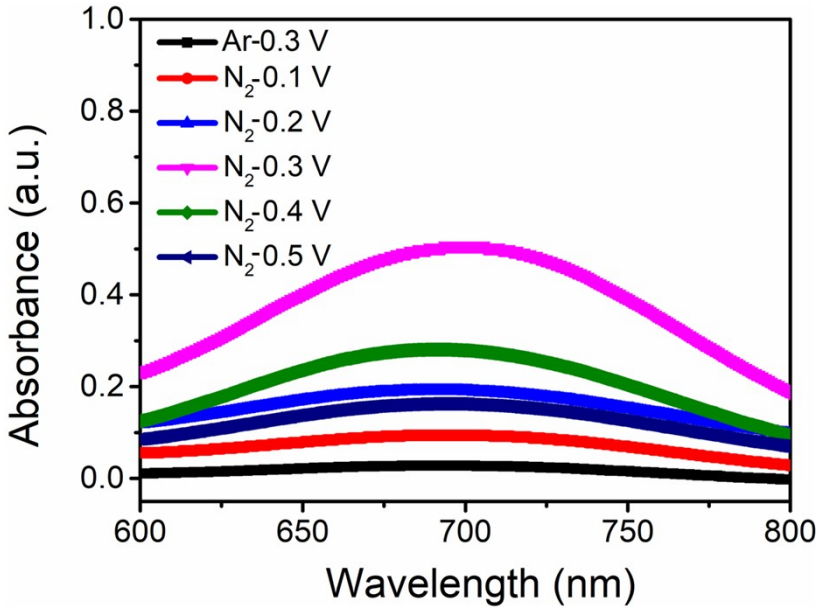

Fig. S10 UV-vis absorbance spectra after potentiostatic tests in 0.1 M Na_2SO_4 at room temperature for the NRR on RO-Cu_3P/CFC electrode.

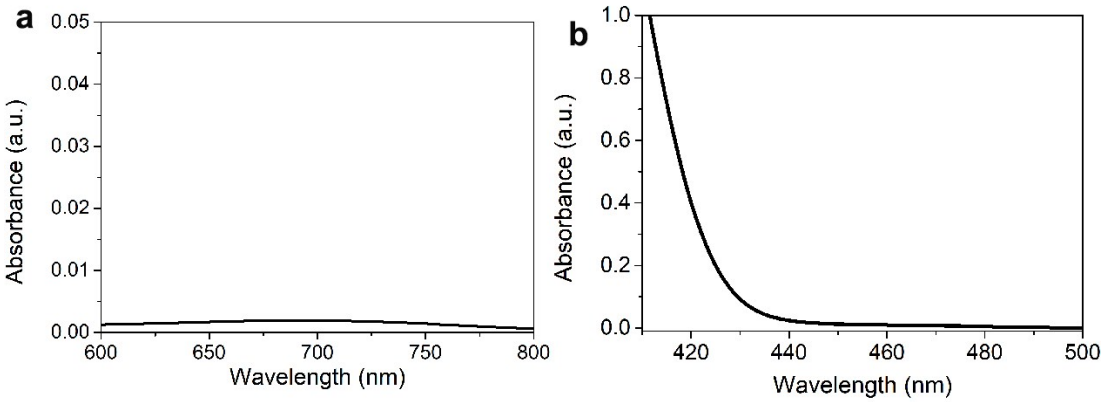

Fig. S11 UV-vis absorbance spectra of the anode compartment after potentiostatic tests at room temperature for the NRR on RO-Cu_3P/CFC electrode.

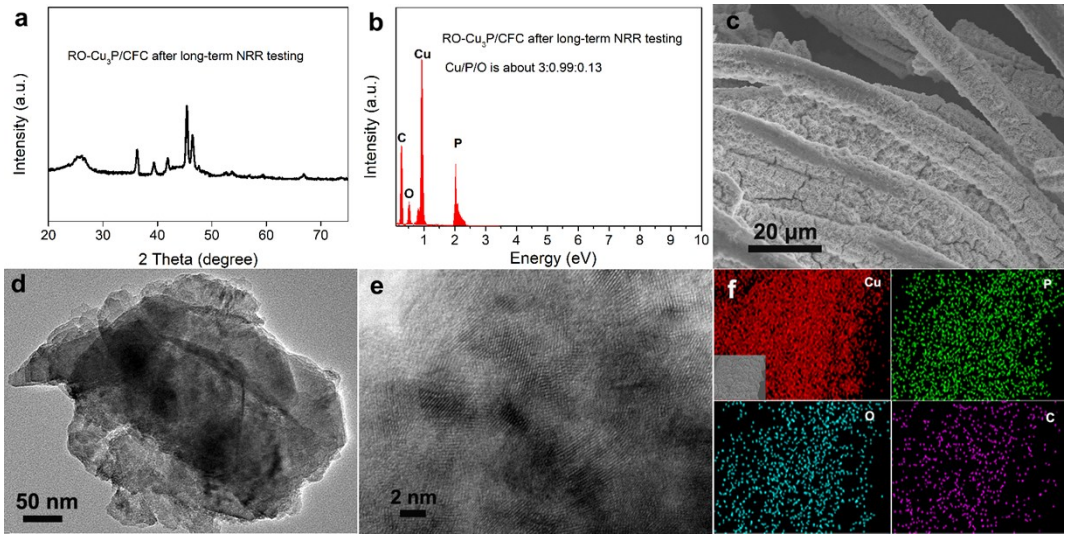

Fig. S12 (a) The XRD patterns of RO-Cu_3P/CFC after long-term NRR testing, (b) the EDX spectra in elemental composition of RO-Cu_3P/CFC after long-term NRR testing, (c) the SEM image of RO-Cu_3P/CFC after long-term NRR testing, the TEM image (d) and HRTEM image (e) of RO-Cu_3P/CFC after long-term NRR testing, (f) the SEM-EDS elemental mapping images of RO-Cu_3P/CFC after long-term NRR testing.

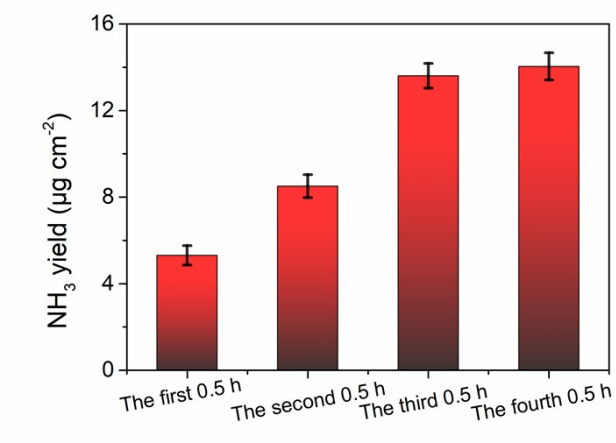

Fig. S13 The ammonia yield of the prepared O-Cu_3P/CFC electrode within two hours.

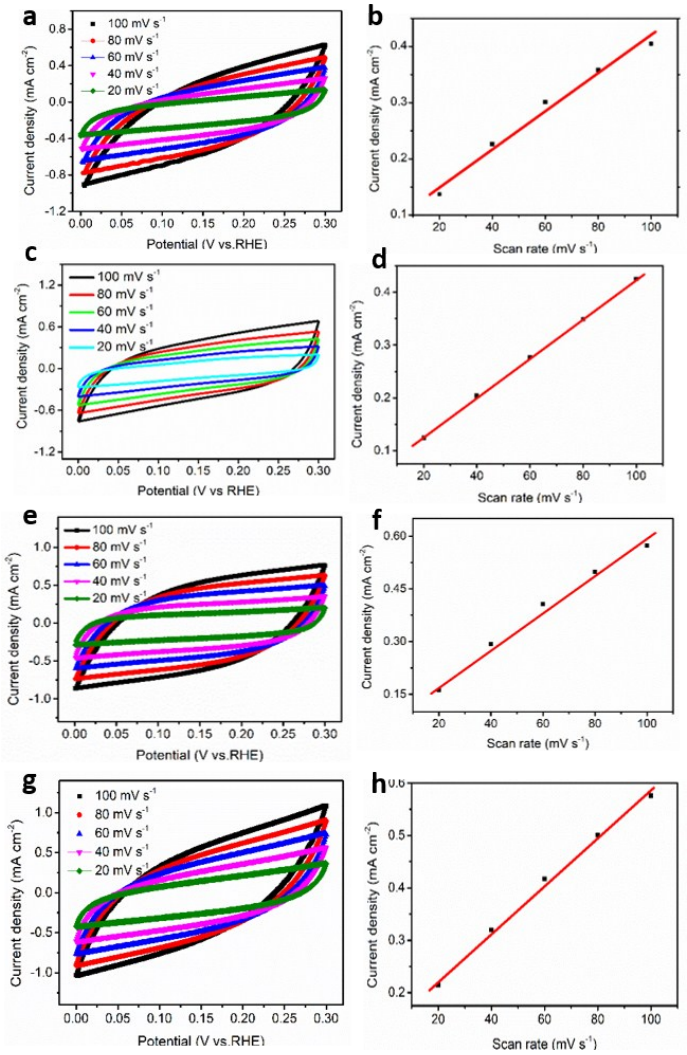

Fig. S14 Determination of double-layer capacitance for the Cu/CFC (a, b), Cu_2O/CFC (c, d), Cu_3P/CFC (e, f) and RO-Cu_3P/CFC (g, h) electrodes in 0.1 M Na_2SO_4 (pH=3) electrolyte. (a, c, e, g), CVs taken over a range of scan rates, (b, d, f, h), Current due to double-layer charging plotted against CV scan rate.

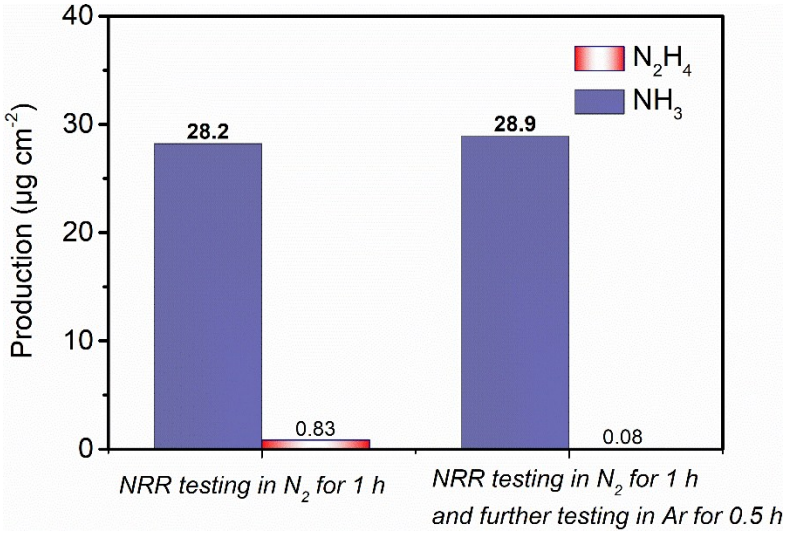

Fig. S15 The NH_3 and N_2H_4 production rate on RO-Cu_3P/CFC electrode of NRR testing in N_2 flow for 1 h, and NRR testing in N_2 flow for 1 h and further testing in Ar for 0.5 h.

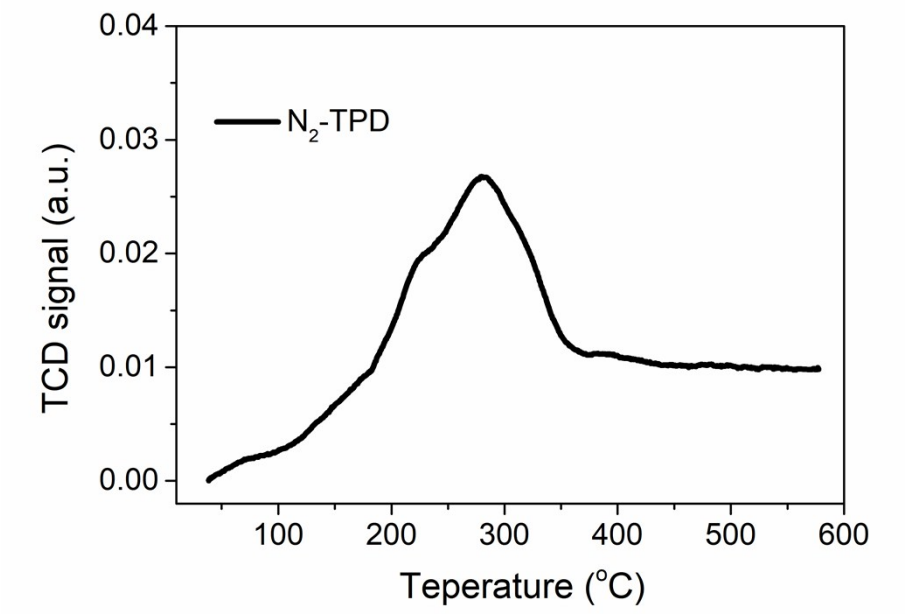

Fig. S16 The N_2-temperature-programmed desorption (N_2-TPD) of RO-Cu_3P/CFC electrode.

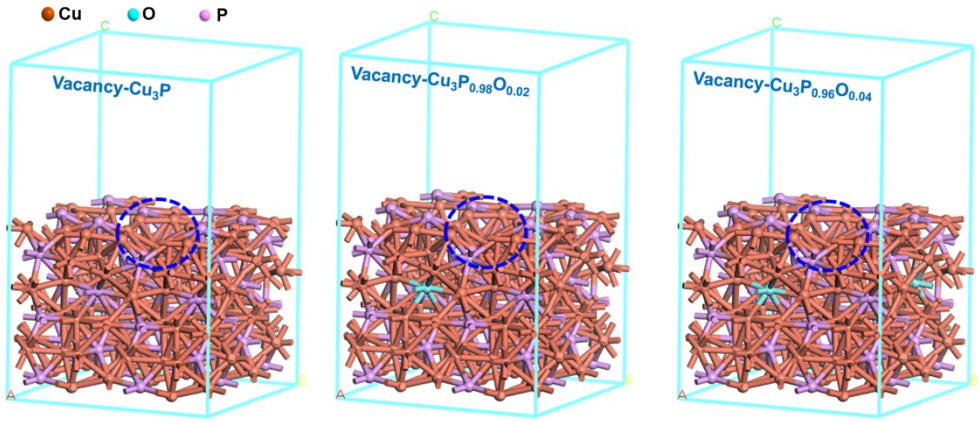

Fig. S17 The calculated crystal structure diagram of surface vacancy Cu_3P, $Cu_3P_{0.98}O_{0.02}$ and $Cu_3P_{0.96}O_{0.04}$.

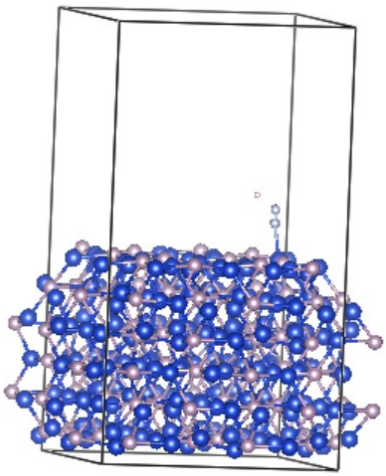

Fig. S18 The optimized Cu_3P structure sites with NRR intermediate states *NNH.

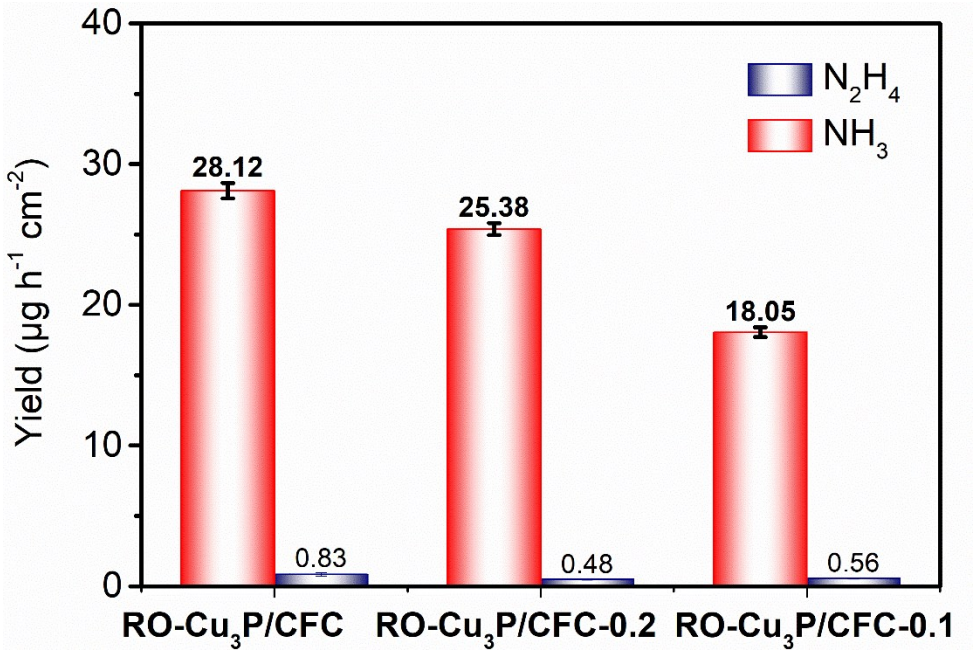

Fig. S19 The NH_3 and N_2H_4 production rate on RO-Cu_3P/CFC, RO-Cu_3P/CFC-0.1 and RO-Cu_3P/CFC-0.2 electrodes.